International Journal for Vitamin and Nutrition Research
Original Communication

Int. J. Vitam. Nutr. Res. **2025**; 95(5): 37275
https://doi.org/10.31083/IJVNR37275

Vitamin K2 Alleviates Metabolic Dysfunction-Associated Steatotic Liver Disease Through Mitochondrial Dysfunction Modulation via Gut Microbiota

Wenchen Wang[1,†], Jia Li[2], Ling Mu[2], Yidan Bai[2], Mengyao Zhu[2], Yaning Zhao[2], Shanbo Hu[2], Jingya Wang[2], Pei Shao[2,*], Xiangni Su[2,3,*,†]

[1]Department of Thoracic Surgery, Tangdu Hospital, Air Force Medical University of People's Liberation Army, 710032 Xi'an, Shaanxi, China
[2]Department of Nursing, The Air Force Medical University of People's Liberation Army, 710032 Xi'an, Shaanxi, China
[3]Department of Clinical Immunology, Xijing Hospital, Air Force Medical University of People's Liberation Army, 710032 Xi'an, Shaanxi, China
*Correspondence: peipeisweet@163.com (Pei Shao); xiangni1013@fmmu.edu.cn (Xiangni Su)
[†]These authors contributed equally.
Academic Editor: Torsten Bohn
Submitted: 9 January 2025 Revised: 27 April 2025 Accepted: 29 May 2025 Published: 23 October 2025

Abstract

Introduction: Metabolic dysfunction-associated steatotic liver disease (MASLD) affects approximately one-third of the global population. Meanwhile, the development of MASLD is related to dysbiosis of the gut microbiota (GM). Our previous studies have shown that Vitamin K2 (VK2) has considerable potential to ameliorate mitochondrial dysfunction in mice fed a high-fat diet (HFD); however, the mechanism through which VK2 improves mitochondrial function and mitigates MASLD remains unclear. **Objective**: This study aimed to elucidate the mechanism through which VK2 modulates MASLD. **Methods**: A total of 80 C57BL/6J mice (4–5 weeks old) were fed a HFD for 16 weeks to establish the MASLD animal model. Additionally, VK2 was administered at a dose of 120 mg/kg/day for the last 8 weeks; 30 mice were fed a normal diet for the entire 24-week period. Mice were randomly divided into groups according to different experimental protocols. Hematoxylin and Eosin (H&E) staining, Oil Red O staining, and Cluster of Differentiation 11b (CD11b) immunofluorescence staining were used to detect liver histology and inflammatory cell infiltration in the mouse liver tissues. Moreover, 16S rRNA gene sequencing, antibiotic treatment, and fecal microbiota transplantation (FMT) were employed to investigate the microbiota-mediated anti-MASLD effects of VK2. Adeno-associated virus 9 (AAV9) was used to elucidate the mechanism through which VK2 regulates MASLD severity. **Results**: VK2 significantly reduced hepatic lipid (triacylglycerol (TG) and total cholesterol (TC)) levels, as well as serum alanine aminotransferase (ALT) and aspartate aminotransferase (AST) levels in HFD-fed mice ($p < 0.05$). VK2 also significantly suppressed inflammatory responses ($p < 0.05$), oxidative stress ($p < 0.05$), and improved mitochondrial dysfunction ($p < 0.05$) in a GM-dependent manner. Furthermore, VK2 restored the balance in the intestinal microbiota primarily through regulating *Lactobacillus* spp. abundance, and markedly alleviated MASLD via a GM-dependent manner. VK2 notably upregulated the expression of SIRT3 signaling pathway proteins ($p < 0.05$), thereby reducing MASLD-associated mitochondrial dysfunction ($p < 0.05$). **Conclusions**: VK2 exerts promising therapeutic effects mainly through enhancing intestinal *Lactobacillus* abundance and ameliorating mitochondrial dysfunction.

Keywords: Vitamin K2; MASLD; mitochondrial dysfunction; gut microbiota; SIRT3 signaling pathway

1. Background

Metabolic dysfunction-associated steatotic liver disease (MASLD) is the primary cause of chronic liver diseases. It affects 25–33% of the global population, thereby posing a significant global health challenge [1]. Metabolic dysfunction-associated steatohepatitis (MASH), a more severe form of MASLD, is related to hepatocellular carcinoma [2]. Several studies have indicated that the gut microbiota (GM) play a crucial role in the etiology and progression of MASLD [3–6]. A prior investigation demonstrated that modulation of the gut microbiome and metabolome with *Lactobacillus* and *Akkermansia* supplement can impede the progression of MASLD [7]. Therefore, interventions targeting the GM may represent a promising therapeutic strategy for inhibiting the development of MASLD.

Vitamins are essential micronutrients for maintaining health by regulating the GM, alleviating oxidative stress, and reducing inflammation and fibrosis [4]. Hence, vitamins are considered the first-line treatment option for treating MASLD, particularly when dietary and other lifestyle changes are insufficient. Vitamin K (VK) plays a critical role in several physiological processes, and its coagulation-unrelated functions have attracted increasing interest among researchers [8]. VK1 and Vitamin K2 (VK2) are two naturally occurring isoforms of VK. VK2 is poorly absorbed into systemic circulation; nevertheless, it can regulate the GM composition to prevent certain diseases [9]. Thus, the beneficial effects of VK2 may be partially attributed to the metabolic activities of the GM [10]. However, the key gut microbial species associated with the beneficial effects of VK2 on MASLD remain elusive.

Our previous studies have revealed that VK2 can remarkably alleviate insulin resistance by improving mitochondrial dysfunction in high-fat diet (HFD)-fed mice [11]. However, the underlying mechanism through which VK2 ameliorates metabolic disorders remains unclear. In the present study, VK2 significantly enriched *Lactobacillus* and improved MASLD-associated mitochondrial dysfunction via the SIRT3 signaling pathway.

2. Materials and Methods

2.1 Animals, Diets, and VK2 Supplementation Protocol

Eighty male C57BL/6J mice (Animal Experiment Center of Air Force Medical University, Xi'an, Shaanxi, China), aged 4–5 weeks, were randomly and equally divided into three groups and subjected to the following treatments: (1) normal diet group (n = 10): the mice were fed a standard chow diet. (2) HFD group (n = 10): the mice were provided with a high-fat diet. (3) HFD + VK2 group (n = 10): in addition to the high-fat diet, VK2 was daily administered via oral gavage at a dose of 120 mg/kg/day for the last eight weeks. The dosage of VK2 intervention was based on our previous research [10]. At the end of the experiment, mice in each group were deeply anesthetized by intraperitoneal injection of ketamine (100 mg/kg) and diazepam (5 mg/kg). Subsequently, liver tissues and blood samples were collected for subsequent analysis.

2.2 Histopathological and Immunofluorescence Staining

H&E staining, Oil Red O staining, and immunofluorescence staining with anti-CD11b antibody (GB11058, 1:100 dilution; Servicebio Technology, Wuhan, China) were conducted on paraffin-embedded and (OCT) compound-embedded frozen liver sections, as previously described in references [11,12].

2.3 Western Blotting

Liver tissues were lysed with radioimmunoprecipitation assay (RIPA) buffer containing 1 mM PMSF (Beyotime Technology, Shanghai, China). Subsequently, the lysates were centrifuged at 14,000 g for 5 minutes. The total protein concentration was quantified using a BCA Protein Assay Kit (Beyotime Technology, Shanghai, China). Loading buffer was added to the protein extract at a final concentration of 5 µg/µL, and the mixture was boiled at 100 °C for 10 minutes to denature the proteins. Equal amounts of protein were separated by electrophoresis on 10% SDS-page gels and then transferred to a PVDF membrane. The membrane was blocked with non-fat milk and then incubated overnight at 4 °C with primary antibodies against SIRT3 (1:1000, 10099-1-AP, Proteintech, Wuhan, Hubei, China), peroxisome proliferator-activated receptor gamma coactivator 1-alpha (PGC-1α) (1:1000, #2178, CST, Beverly, MA, USA), β-Tubulin (1:1000, 80713-1-RR, Proteintech, Wuhan, China), Catalase (1:1000, 21260-1-AP, Proteintech, Wuhan, Hubei, China), and superoxide dismutase 2 (SOD2) (1:1000, 24127-1-AP, Proteintech, Wuhan, Hubei, China). The membranes were washed three times with Tris-buffered saline + Tween 20 (TBST) buffer, followed by a 2-hour incubation with HRP conjugated secondary anti-rabbit (1:1000, #7073, CST) or anti-mouse antibodies (1:1000, #7076, CST). After another three washes with TBST buffer, the blots were visualized using an ECL kit [10].

2.4 Real-Time Quantitative PCR

Total RNA was isolated using the Magen HiPure Universal RNA Kit (R4130-02, Magen Biotechnology, Guangzhou, Guangdong, China), and the RNA concentration was measured with a NanoDrop 2000C spectrophotometer. gDNA was removed from 500 ng of RNA using the gDNA eraser (RR047Q, Takara, Kusatsu, Japan), and then the RNA was reverse-transcribed using the PrimerScript RT Reagent Kit. qPCR targets were normalized to β-Actin, and the relative mRNA levels were determined by calculating the average expression in the control group. Primer sequences were obtained from PrimerBank.

2.5 FMT and Antibiotic Treatment

Donor feces were collected, diluted in deoxygenated saline, and filtered for inoculation into mice. Pseudo-germ-free mice were pre-treated with an antibiotic cocktail for two weeks. Subsequently, these mice were randomly divided into two groups: (1) HFD-HFD group: feces from the HFD group were administered to pseudo-germ-free HFD-fed mice; (2) VK2-HFD group: feces from the VK2 group were administered to pseudo-germ-free mice. The recipient mice were then fed a HFD for an additional 4 weeks [13].

2.6 Adeno-Associated Virus (AAV) Delivery

Twenty HFD-fed mice were intraperitoneally injected with AAV-*shSirt3* (1×10^{12} vg/mL) for three consecutive weeks to establish the *shSirt3* mouse model. Ten HFD-fed mice were intraperitoneally injected with Saav-*shControl* (1×10^{12} vg/mL) for three consecutive weeks to establish the *shControl* mouse model. The *shSirt3* mice were then divided into the following two groups: (1) *shSirt3* + HFD group (n = 10); (2) *shSirt3* + VK2 group (n = 10).

2.7 Mitochondrial Isolation and Oxygen Consumption Rate (OCR) Assays

Immediately after sacrifice, mouse liver tissues were rinsed in cold PBS and homogenized. Mitochondria were isolated through a series of dual centrifugation steps. Freshly isolated liver mitochondria were suspended in mitochondrial assay solution (MAS) [14]. One to three micrograms of mitochondria were transferred to a XFe24 microplate, which was then filled with MAS to a final volume of 500 µL, containing either glutamate/malate or succinate/rotenone. The OCR was measured in response to the sequential injection of ADP, oligomycin, FCCP and antimycin A. The respiratory rates were reported as oxygen flux per unit mass, and all readings were normalized to the micrograms of protein in the mitochondria [10,15].

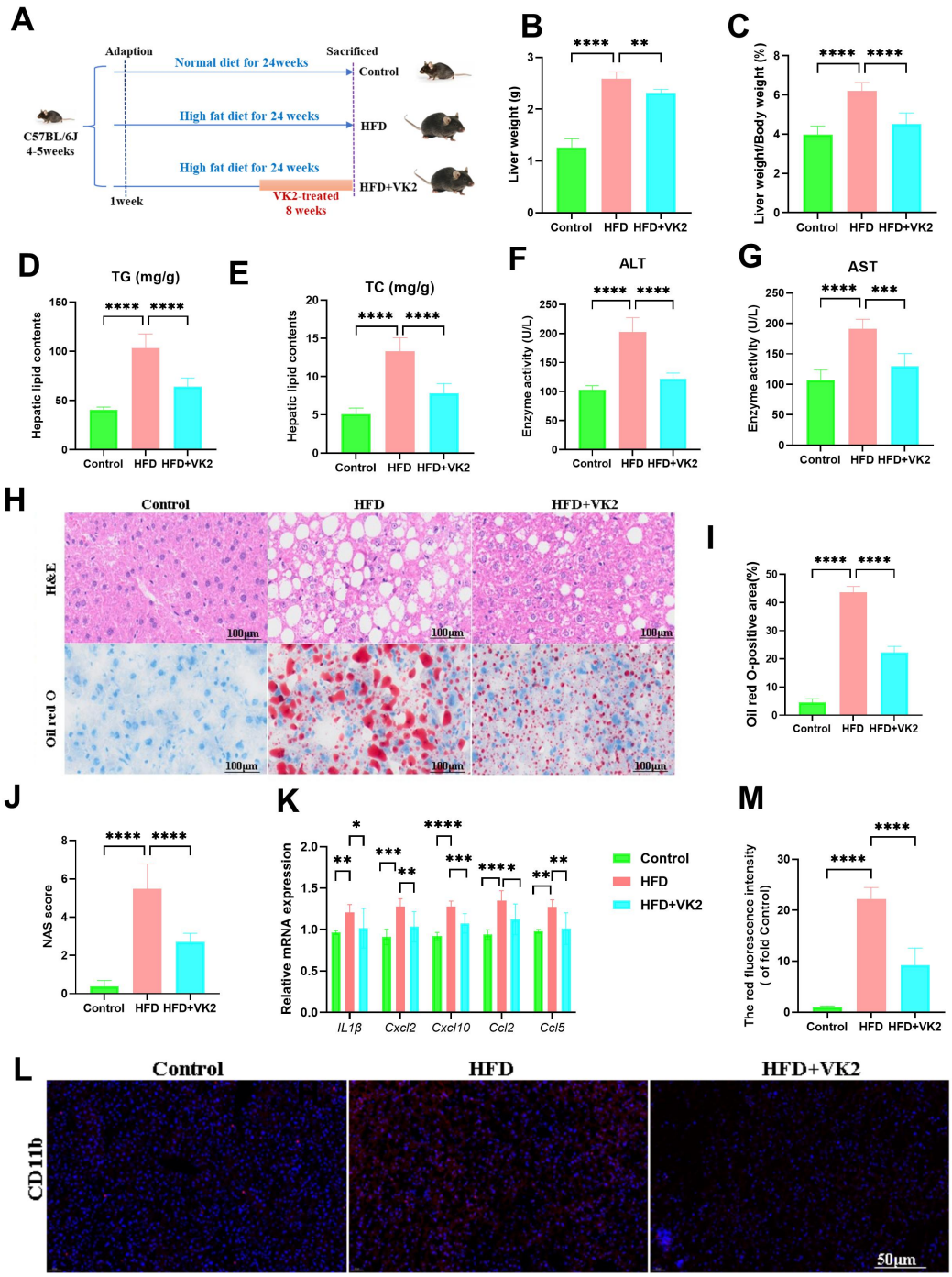

Fig. 1. VK2 attenuates HFD-induced MASLD. (A) Schematic of VK2 gavage intervention. (B,C) LW and LW/BW ratios in all groups. n = 10 per group. (D,E) TG and TC levels in hepatic tissues. n = 10 per group. (F,G) Serum ALT and AST levels. n = 10 per group. (H–J) Representative images of H&E staining, Oil Red O staining, and MASLD activity score to evaluate hepatic steatosis and lipid accumulation. n = 6 per group. Scale bar = 100 μm. (K) Relative mRNA expression levels of inflammatory genes (*IL-1β*, *Cxcl2*, *Cxcl10*, *Ccl2*, *Ccl5*) determined by RT-qPCR, normalized to the *β*-actin-encoding gene *Actb*. n = 6 per group. (L,M) Immunofluorescence staining for CD11b (red, inflammatory cells) in liver tissues, with nuclei counterstained with DAPI (blue). n = 4 per group. Scale bar = 50 μm. Data were analyzed by one-way ANOVA, followed by Tukey's post-hoc test. Significant differences were noted between the control and HFD groups, and between the HFD and VK2-treated groups. *$p < 0.05$; **$p < 0.01$; ***$p < 0.001$; ****$p < 0.0001$. VK2, Vitamin K2; HFD, high-fat diet; MASLD, metabolic dysfunction-associated steatotic liver disease; LW, liver weight; BW, body weight; TG, triacylglycerols; TC, total cholesterol; ALT, alanine aminotransferase; AST, aspartate aminotransferase; RT-qPCR, real-time quantitative PCR.

2.8 Transmission Electron Microscopy

Liver tissue sections (1 mm × 1 mm) were fixed in a 2.5% glutaraldehyde buffer solution at 4 °C for 3 hours. Subsequently, the fixation solution was replaced with a cacodylate buffer containing 0.1 M glutaraldehyde and kept at 4 °C. After washing, dehydration, and resin embedding, the liver tissues were sectioned using an ultramicrotome. The sections were observed under a transmission electron microscope (JEM 1400, JEOL Ltd., Tokyo, Japan), and images were captured at magnifications of 10,000× and 84,000× for the further analysis of mitochondrial density, number, and area [10].

2.9 ATP and SOD2 Detection

The contents of ATP and SOD2 were determined using an ATP Assay Kit (Beyotime, S0026) based on the luciferin/luciferase method and a Superoxide Dismutase Assay Kit with NBT (Beyotime, S0101S), following the manufacturer's instructions. All data were measured with multimode microplate readers (Tecan Infinite 200 PRO, Tecan Life Sciences, Männedorf, Switzerland). Briefly, liver tissue homogenates were centrifuged at 12,000 g for 5 minutes at 4 °C. The supernatant was collected and used for the detection of ATP and SOD2 levels. The luminescence was measured using multimode microplate readers (Tecan Infinite 200 PRO).

2.10 Mitochondrial Respiratory Complex Activity Assay

Mitochondria were extracted from fresh liver tissues, and the activities of mitochondrial respiratory complexes I and IV were measured using the corresponding kits from Abcam MitoSciences (Cambridge, UK) according to the manufacturer's instructions.

2.11 Statistical Analysis

Appropriate statistical methods were employed using SPSS software (Version 22, IBM Corp., Armonk, NY, USA). One-way and two-way ANOVA were conducted for multiple comparisons, while Student's *t*-test was utilized for comparisons between two groups. A p value of less than 0.05 was considered statistically significant.

3. Results

3.1 VK2 Attenuates HFD-Induced MASLD

To investigate the effects of VK2 on MASLD, C57BL/6J mice were fed a HFD for 16 weeks, followed by oral administration of VK2 (120 mg/kg/day) while continuing the HFD for an additional 8 weeks (Fig. 1A). Compared with the control group, HFD-fed mice exhibited a significant increase in body weight over time. Both liver weight (LW) and the LW-to-body weight (LW/BW) ratio were significantly lower in the VK2-treated group when compared to the HFD group (Fig. 1B,C). Hepatic triglyceride (TG) and total cholesterol (TC) levels were also significantly reduced in VK2-treated mice (Fig. 1D,E). Given that lipotoxicity can lead to hepatocyte injury or death [16], serum alanine aminotransferase (ALT) and aspartate aminotransferase (AST) levels were elevated after 24 weeks of HFD feeding. However, VK2 treatment significantly lower serum ALT and AST levels compared to the HFD group (Fig. 1F,G). Hepatic histology revealed that VK2 reduced HFD-induced hepatic ballooning and lipid droplet accumulation (Fig. 1H–J). VK2 treatment suppressed the expression of inflammatory genes (*IL-1β*, *Cxcl2*, *Cxcl10*, *Ccl2*, *Ccl5*) (Fig. 1K). Additionally, CD11b immunofluorescence staining showed that VK2 significantly decreased inflammatory cell infiltration in the liver tissues of HFD-fed mice (Fig. 1L,M). Collectively, these findings indicate that VK2 treatment ameliorates the progression of HFD-induced MASLD.

3.2 VK2 Improves Oxidative Stress and Mitochondrial Function in HFD-Fed Mice

Mitochondrial dysfunction contributes to MASLD progression. Increased free fatty acid (FFA) influx into hepatocytes induces metabolic changes that impair mitochondrial function [17]. VK2 treatment significantly reduced HFD-induced reactive oxygen species (ROS) production, as measured by DCFH-DA staining (Fig. 2A,B). Furthermore, VK2 treatment significantly enhanced ATP content, mitochondrial-DNA (mtDNA) gene expression, and SOD2 enzyme activity, suggesting that VK2 alleviated oxidative stress in HFD-fed mice (Fig. 2C–E). To further assess mitochondrial function, we measured bioenergetic parameters. Compared with the HFD group, VK2 treatment enhanced overall mitochondrial activity in the liver, restoring mitochondrial dysfunction and improving basal respiration and spare respiratory capacity in HFD-fed mice (Fig. 2F–K). Transmission electron microscopy (TEM) revealed that HFD-fed mice exhibited abnormal mitochondria with displaced myofibrils, swelling, and vacuole-like degeneration compared to the control group (Fig. 2L). In contrast, VK2-treated mice showed a significant increase in the total number and a decrease in average mitochondria area (Fig. 2M,N). Consistently, VK2 treatment upregulated the expression of mitochondrial biogenesis genes (Fig. 2O). Collectively, these findings indicate that VK2 ameliorates mitochondrial dysfunction and oxidative stress.

3.3 VK2 Mitigates Gut Dysbiosis in HFD-Induced MASLD

Given that the GM contributes to MASLD progression, we investigated the effect of VK2 treatment on GM composition. Compared with the HFD group, the VK2-treated group exhibited a significant increase in the Ace and Shannon indices (Fig. 3A,B), indicating that VK2 treatment restored reduced gut microbial diversity in HFD-fed mice. UniFrac-based principal coordinate analysis (PCoA) and partial least squares-discriminant analysis (PLS-DA) revealed distinct clustering of microbial communities among groups (Fig. 3C,D). The relative abundance of bacterial species *Lactobacillus*

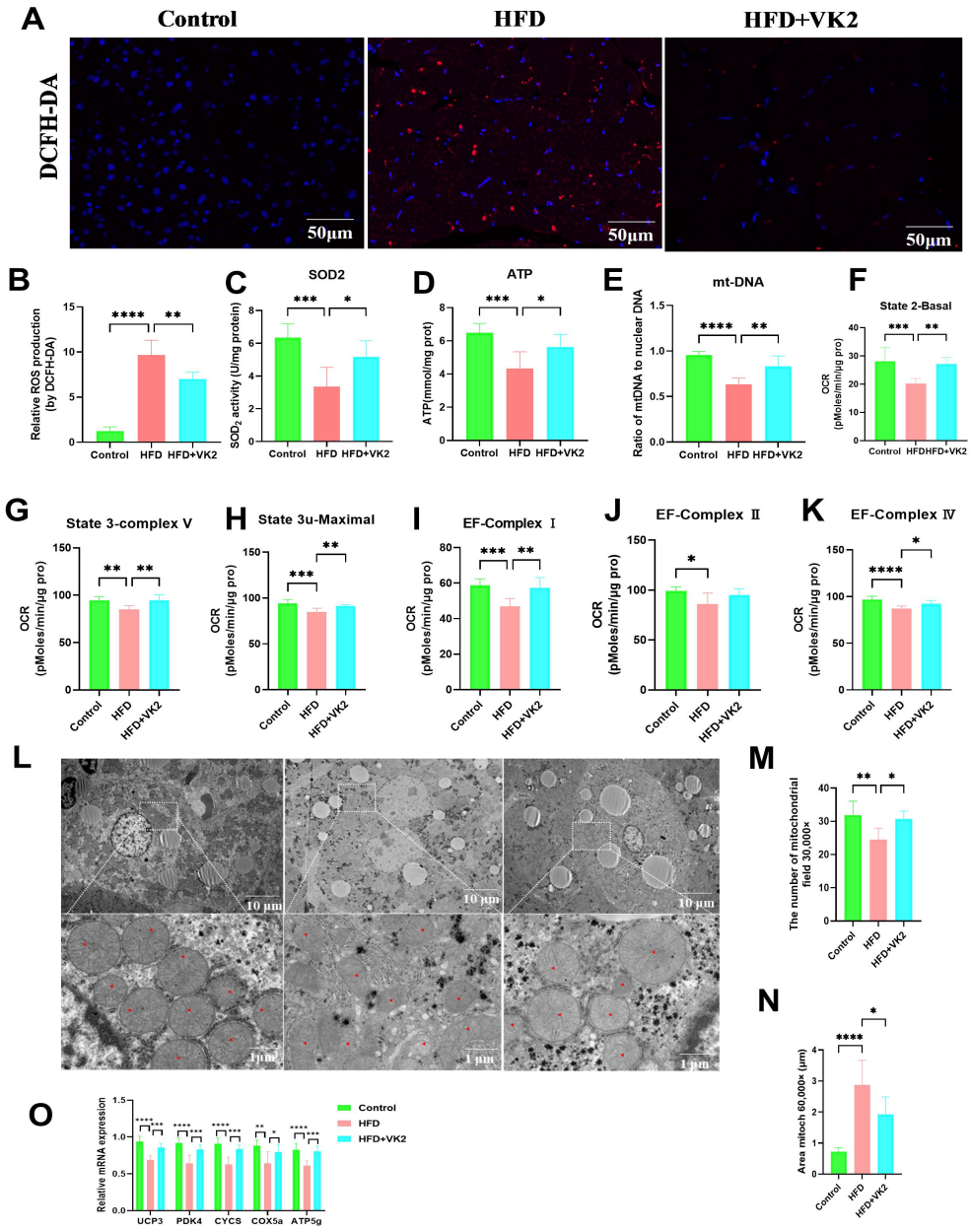

Fig. 2. VK2 improves oxidative stress and mitochondrial function in HFD-fed mice. (A,B) Hepatic reactive oxygen species (ROS) levels measured by DCFH-DA staining and quantification of relative ROS production. n = 6 per group. Scale bar = 50 μm. (C–E) Hepatic superoxide dismutase 2 (SOD2) enzyme activity (C), ATP content (D), and mitochondrial DNA (mtDNA) copy number (mtDNA/nuclear DNA ratio) (E) in the liver tissue. n = 7 per group. (F–K) Oxygen consumption rate (OCR) of isolated liver mitochondria to assess mitochondrial bioenergetic. Basal respiration was measured under State 2 (F), State 3 (G), and State 3u (H) conditions. Electron transport chain complex activity was determined for complex I (I), complex II (J), and complex IV respiration (K). n = 6 per group. (L) Transmission electron microscopy (TEM) images of hepatic mitochondria (red triangle indicate mitochondrial structures). Images were acquired at 10,000× and 84,000× magnifications. Scale bars = 10 μm (low magnification) and 1 μm (high magnification). (M,N) Quantification of mitochondrial number and average area per cell using ImageJ software (Version 1.8.0.112, Madison, WI, USA). (O) Relative mRNA expression levels of mitochondrial biogenesis genes measured by RT-qPCR. n = 8 per group. Data are presented as mean ± standard deviation (SD). One-way ANOVA with Tukey's post-hoc test was used for multiple-group comparisons. Significant differences were noted between the control and HFD groups, and between the HFD and VK2-treated groups. *$p < 0.05$; **$p < 0.01$; ***$p < 0.001$; ****$p < 0.0001$.

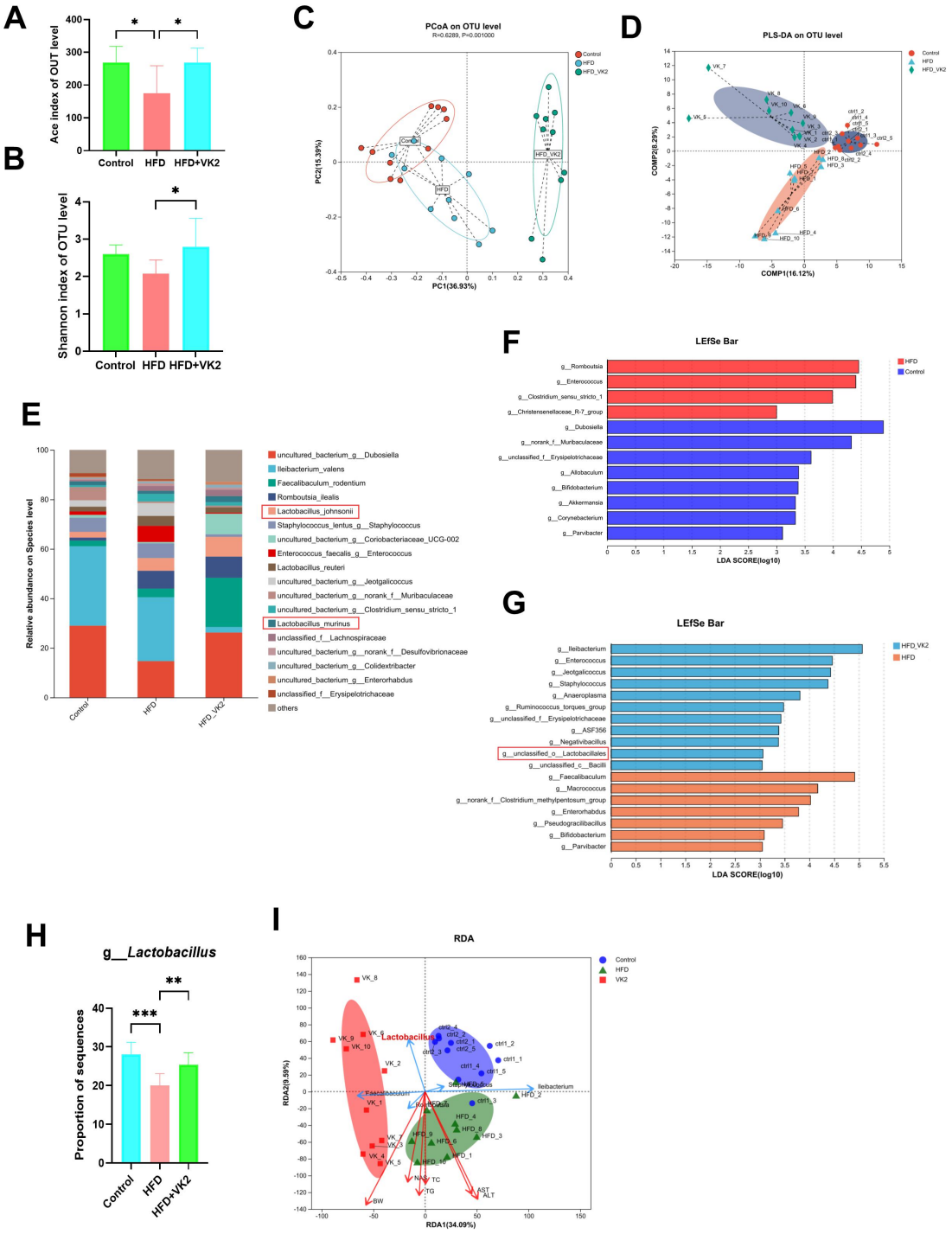

Fig. 3. VK2 mitigates gut dysbiosis in HFD-induced MASLD. Fresh fecal samples were collected from mice after 4 weeks of VK2 treatment for 16S rRNA gene sequencing analyses. (A) Ace and (B) Shannon diversity indices of the GM. (C,D) Weighted UniFrac PCoA analysis and PLS-DA analysis of microbial communities. (E) Relative abundance of bacterial genera at the genus level. (F,G) LEfSe was used to identify differentially abundant taxa in the GM. (H) Relative abundance of *Lactobacillus* across all groups. (I) RDA analysis of the correlation between *Lactobacillus* and MASLD-associated parameters. All data are expressed as mean ± SEM. *p* values shown in Fig. 3A,B,H were determined by one-way ANOVA with Dunnett's post hoc test (comparison against the control group). Significant differences were noted between the control and HFD groups, and between the HFD and VK2-treated groups. $*p < 0.05$; $**p < 0.01$; $***p < 0.001$. GM, gut microbiota; PCoA, principal coordinate analysis; PLS-DA, partial least squares-discriminant analysis; LEfSe, linear discriminant analysis effect size; RDA, redundancy analysis.

johnsonii and *Lactobacillus murinues* were significantly increased by VK2 treatment compared with the HFD group (Fig. 3E) [18]. To identify specific bacterial taxa altered by VK2 supplementation, linear discriminant analysis (LDA) effect size (LEfSe) was utilized to compare the fecal microbiota composition at the genus level. Compared with the control group, HFD group showed lower abundance of *Dubosiella*, *norank_f__Muribaculaceae*, *unclassified_f__Erysipelotrichaceae Allobaculum*, *Bifidobacterium*, *Akkermansia*, *Corynebacterium*, *Parvibacter* but a higher abundance of *Rombountsia*, *Enterococcus*, *Clostridium_sensu_stricto_1*, *Christensenellanceae_R-7_group* (Fig. 3F). Conversely, the HFD group enriched *Ileibacterium*, *Enterococcus*, *Jeotgalicoccus*, *Staphylococcus*, *Anaeroplasma*, *Ruminococcus_torques_group*, *unclassified_f_Erysipelotrichaceae*, *ASF356*, *Negativibacillus*, *unclassified_c_Lactobacillales*, *unclassified_c_Bacilli*, whereas VK2 treatment increased the abundance of *Faecalibaculum*, *Macrococcus*, *norank_f__Clostridium_methylpentosum_group*, *Enterorhabdus*, *Pseudogracilibacillus*, *Bifidobacterium*, *Parvibacter* in HFD-fed mice (Fig. 3G). At the genus level, the HFD group exhibited a significant decrease in *Lactobacillus* relative abundance compared with the control group, whereas VK2 treatment significantly restored *Lactobacillus* abundance (Fig. 3H). Redundancy analysis (RDA) showed that *Lactobacillus* was significantly negatively correlated with MASLD-associated parameters (hepatic TC, TG, serum ALT, AST, and NAS score) (Fig. 3I); suggesting that *Lactobacillus* enrichment may be mediate the protective effects of VK2 against MASLD. Collectively, these results indicate that VK2 reverses gut dysbiosis in HFD-induced MASLD.

3.4 VK2 Attenuates MASLD in a GM-Dependent Manner

To determine whether the beneficial effects of VK2 in HFD-fed mice are dependent on the GM, we transplanted fecal microbiota from VK2-treated HFD-fed donor mice to recipient HFD-fed mice via daily gavage. Recipient mice were pre-treated with broad-spectrum antibiotics in drinking water for 2 weeks to generate conditionally pseudo germ-free mice (Fig. 4A). Following the fecal microbiota transplantation (FMT), recipient mice that received VK2-treated microbiota exhibited significantly lower NAS scores (Fig. 4B,C), accompanied by reduced hepatic lipid levels (TC and TG) (Fig. 4D,E), decreased serum AST and ALT levels (Fig. 4F,G), and enhanced SOD2 activity (Fig. 4H) and mitochondrial respiratory complex I and IV activity (Fig. 4I,J). These findings demonstrated that fecal microbiota transplantation (FTM) from VK2-treated donor recapitulated the beneficial effects of VK2, including reduced oxidative stress and improved mitochondrial function in the liver of HFD-fed mice. Collectively, these data indicate that VK2 ameliorates MASLD via a GM-dependent mechanism.

3.5 VK2 Improves Mitochondrial Activity Through SIRT3 Signaling Pathway

Our previous studies have revealed that VK2 can significantly alleviate insulin resistance by improving mitochondrial dysfunction in HFD-fed mice via SIRT3 signaling. To determine whether SIRT3 mediates the effect of VK2 on mitochondrial function *in vivo*, we knocked down the gene encoding SIRT3 in the livers of mice by delivering shRNA using adeno-associated virus 9. *SIRT3* knockdown reduced the effect of VK2 on the LW/BW ratio (Fig. 5A,B), activities of AST and ALT (Fig. 5C,D), and hepatic lipid levels (TG and TC) (Fig. 5E,F). Moreover, the ATP level and SOD2 enzyme activity were not significantly improved by VK2 treatment in HFD-fed mice with *SIRT3* knockdown (Fig. 5G,H). Additionally, VK2 did not enhance the mitochondrial basal respiration and spare respiratory capacity in HFD-fed mice with *SIRT3* knockdown (Fig. 5I–N). VK2 treatment increased the protein expression levels of SIRT3, SOD2, and catalase in the liver tissues of HFD-fed mice (Fig. 5O,P). However, *SIRT3* knockdown abolished the effect of VK2 on mitochondrial function and the protein expression of SIRT3, peroxisome proliferator-activated receptor gamma coactivator 1-alpha (PGC-1α), SOD2 and catalase (Fig. 5Q,R). These findings revealed that SIRT3 plays a critical role in the protective effects of VK2 on MASLD.

4. Discussion

MASLD is the leading chronic liver disease worldwide. The GM has been recognized as a key mediator in the pathogenesis and progression of MASLD, primarily through regulation host energy metabolism and metabolic homeostasis [19,20]. Although previous studies have shown that VK2 acts as an effective antioxidant and anti-inflammatory micronutrient in treating HFD-induced insulin resistance [10], the underlying mechanisms by which VK2 exerts its effects remain poorly understood, and whether VK2 functions through a GM-dependent mechanism has not been explored. The present study demonstrated that VK2 significantly ameliorated mitochondrial dysfunction in HFD-fed mice by regulating the GM, particularly by increasing the abundance of *Lactobacillus*. VK2 treatment significantly activated the SIRT3 signaling pathway, thereby mediating the alleviation of mitochondrial dysfunction.

Vitamins have well-established roles in bacterial metabolism. VK is a less understood mediator of both vitamin-GM interactions and community dynamics. The VK requirement in humans is met through the diet, which may involve the influence on the composition of GM by dietary components [21]. VK1 is present in leafy green vegetables [22]. VK2 is present in dairy products and fermented foods [23], menaquinone-4 (MK-4) is a homolog of VK2, is the major form of VK in animal tissues and is produced by the GM [24]. The relevance of MK-4 produced by gut bacteria to human health has long been speculated [25]. VK act as a cofactor for the carboxylation of VK-dependent

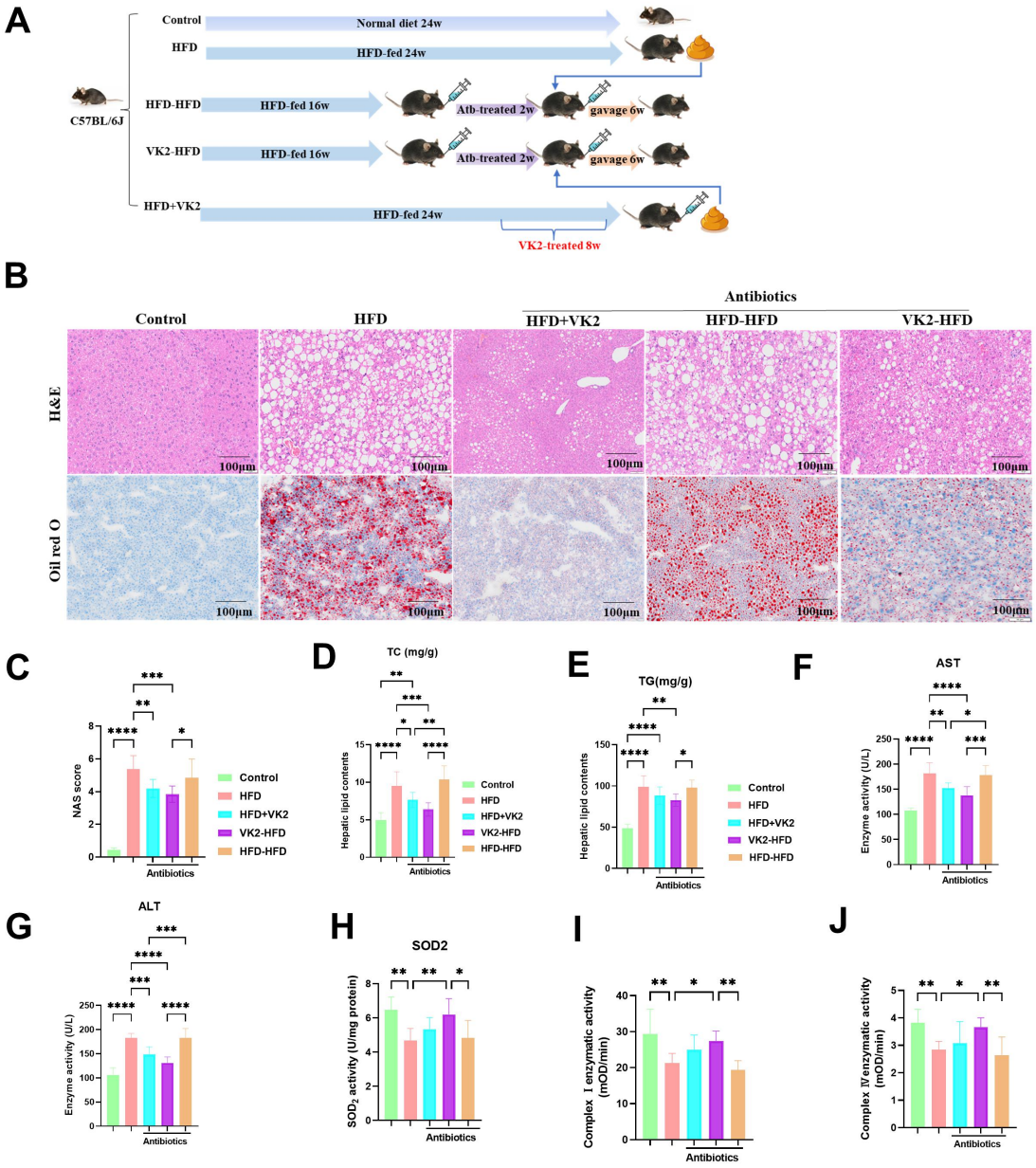

Fig. 4. VK2 attenuates MASLD in a GM-dependent manner. (A) Schematic of the FTM study. (B,C) H&E staining and Oil Red O staining were used to determine hepatic steatosis and lipid accumulation, and the MASLD activity score. n = 6 per group. Scale bar = 100 μm. (D,E) Hepatic TG and TC levels. n = 10 per group. (F,G) Serum ALT and AST levels. n = 10 per group. (H) Hepatic SOD2 activity was measured. n = 7 per group. (I,J) Activity of hepatic mitochondrial respiratory complex I and IV. n = 7 per group. One-way ANOVA was used to analyze data. Significant differences were observed between the control and HFD-fed groups, and between the HFD group and the groups treated with VK2 along with antibiotics plus HFD or the FMT group. *$p < 0.05$; **$p < 0.01$; ***$p < 0.001$; ****$p < 0.0001$.

proteins, which are involved in diverse functions [26]. Historically, gut bacteria have been considered to contribute up to 50% of the host's VK requirement. However, the underlying mechanisms by which VK alleviates mitochondrial dysfunction and exerts an anti-inflammatory effect remain elusive [27]. Additionally, a previous study demonstrated that vitamin B12 is similarly metabolized by gut bacteria and serves as a modulator of gut microbial ecology [28]. Collectively, these findings enhance our understanding of micronutrient-microbiota interactions.

VK2 functions as an electron carrier in bacterial respiration [9]. Mice with VK deficiency exhibited lower relative abundance of *Lactobacillus* than those fed a VK2-supplemented diet [9]. *Lactobacillus* species are known to enhance the intestinal epithelial barrier function and tight junction integrity, thereby playing a beneficial role in pro-

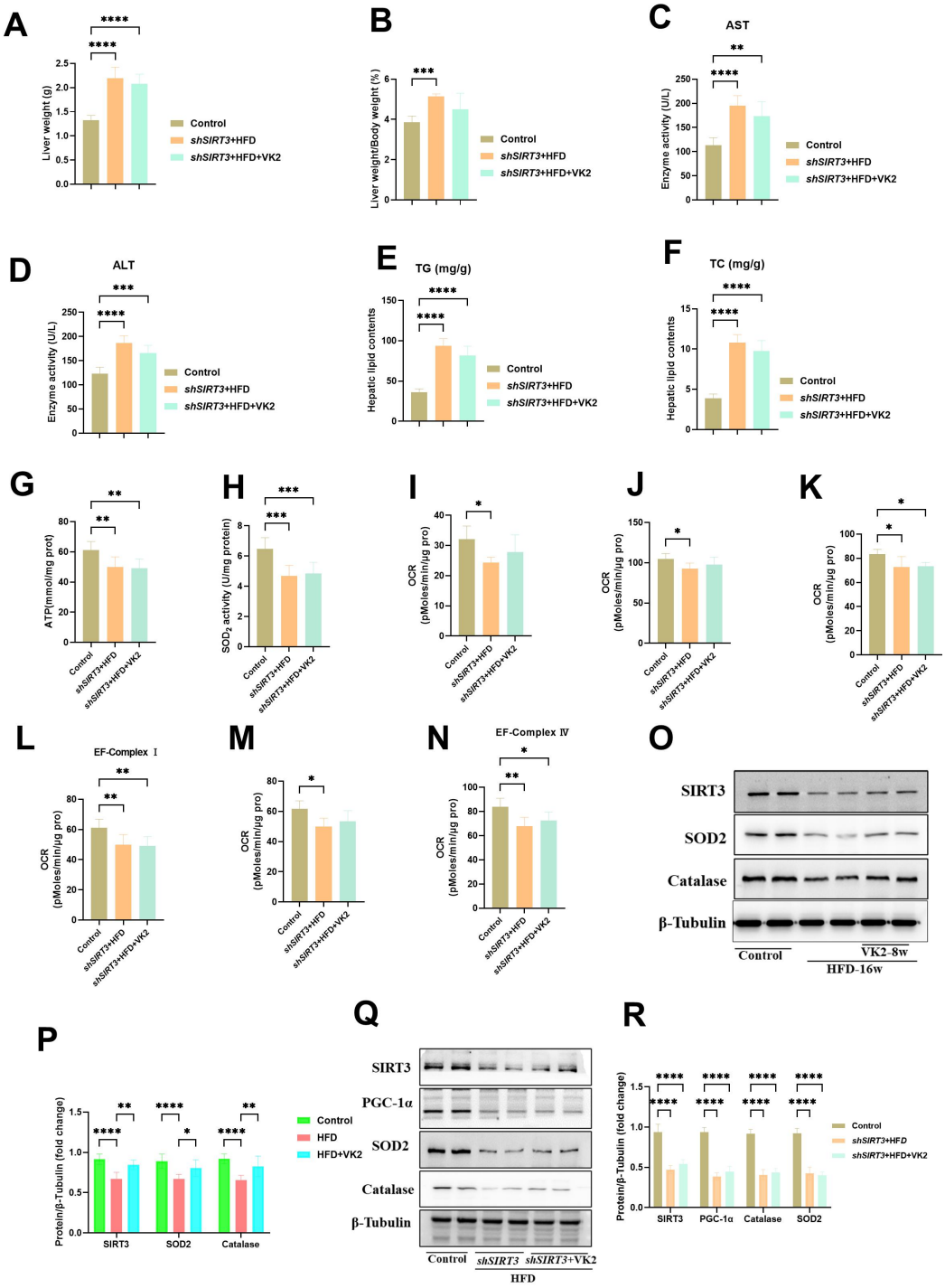

Fig. 5. VK2 improves mitochondrial activity through SIRT3 signaling pathway. (A,B) LW and the LW/BW ratio. (C,D) Serum ALT and AST levels. n = 10 per group. (E,F) TG and TC levels. n = 8 per group. (G,H) Hepatic ATP contents and SOD2 enzyme activity. n = 7 per group. (I–N) OCR of isolated liver mitochondria to assess mitochondrial bioenergetic. Basal respiration was measured under State 2 (I), State 3 (J), and State 3u (K) conditions. Electron transport chain complex activity was determined for complex I (L), complex II (M), and complex IV (N). n = 6 per group. (O,P) Protein expression of SIRT3, SOD2 and catalase were determined in all groups. n = 7 per group. (Q,R) Protein expression of SIRT3, PGC-1α, SOD2, and catalase in control and the *shSIRT3* + HFD, and the VK2-treated *shSIRT3* + HFD groups. n = 6 per group. Data were analyzed by one-way ANOVA followed by Tukey's post-hoc test. Significant differences were observed between the control and the *shSIRT3* + HFD, and the VK2-treated *shSIRT3* + HFD groups. *$p < 0.05$; **$p < 0.001$; ***$p < 0.001$; ****$p < 0.0001$. PGC-1α, peroxisome proliferator-activated receptor gamma coactivator 1-alpha.

tecting the gut mucosal barrier [29,30]. Species *Lactobacillus* strains, such as *L. rhamnosus*, *L. acidophilus*, and *L. bulgaricus*, have been shown to reduce serum transaminase levels, alleviate hepatic steatosis, and decrease the MASLD activity score (NAS) [29,30]. Additionally, other *Lactobacillus* species (e.g., *L. gasseri*) exert protective effects by mitigating tight junction proteins disruption and enhancing intestinal barrier function [31,32]. Our study revealed that VK2 supplementation exerts a novel role in modulating GM composition, whereby VK2 administration enriches the relative abundance of *Lactobacillus* and alleviates MASLD-related pathological phenotypes in HFD-fed mice. These findings align with previous reports of GM composition changes following VK supplementation and highlight the critical role of the microbiota in mediating VK2's therapeutic effects against MASLD.

In this study, VK2 treatment upregulated hepatic SIRT3 protein expression. SIRT3 plays protective role in aging, diabetes, obesity, hypertension, and MASLD [33–35]. Consistent with these observations, SIRT3 knockdown abolished the beneficial effects of VK2 on oxidative stress and mitochondrial dysfunction. Mechanistically, VK2 treatment significantly enriched the commensal bacterium *Lactobacillus* and activated the SIRT3 signaling pathway, linking microbial modulation to mitochondrial protection.

Our research first demonstrated that VK2 improves mitochondrial dysfunction in HFD-fed mice by activating the SIRT3 signaling pathway and alleviates HFD-induced MASLD through GM regulation, particularly by increasing the abundance of *Lactobacillus*. However, several limitations merit consideration. First, while our study revealed that VK2's effect on mitochondrial function may be correlated with other mitochondrial pathway (e.g., AMPK signaling cascades), we only characterized the SIRT3 signaling-dependent beneficial effects. Second, although we focused on VK2-mediated enrichment of *Lactobacillus*, the role of gut microbial metabolites in this process remains unexplored and could be further investigated using high-resolution mass spectrometry. Third, we did not include a normal diet group treated with VK2 to rule out the potential impact of VK2 itself on normal liver. Additionally, the effect of *Lactobacillus* supplementation alone on HFD-fed mice MASLD mice was not examined, which would help clarify the causal role of this genus in VK2's therapeutic effects.

5. Conclusions

The current study demonstrated that Vitamin K2 (VK2) significantly ameliorated the symptoms of MASLD through a GM dependent mechanism. VK2 treatment rectified the microbial dysbiosis and alleviated MASLD by activating the SIRT3 signaling pathway. Additionally, VK2 treatment reduced MASLD symptoms by enhancing the abundance of beneficial *Lactobacillus* species, thereby promoting their dominant colonization within the intestinal tract. Collectively, these results uncover a novel role of VK2 in the context of MASLD. The findings of this research may offer a promising therapeutic strategy for the treatment of MASLD by targeting key microbial metabolites or specific gut bacterial species.

Availability of Data and Materials

The authors confirm that the data supporting the findings of this study are available within the article.

Author Contributions

XS: Investigation, Writing—review & editing, Funding acquisition, Project administration, Supervision. PS and WW: Data curation, Writing—original draft, Formal analysis. JL, LM, YB and MZ: Reviewing, Data analysis and Interpretation as well as Writing—original draft. SH, YZ and JW: Methodology and drafting the manuscript. All authors read and approved the final manuscript. All authors have participated sufficiently in the work and agreed to be accountable for all aspects of the work.

Ethics Approval and Consent to Participate

All procedures performed in studies involving animals were in accordance with the ethical standards of Ethics Committee in the Air Force Medical University (NO. IACUC20141259).

Acknowledgment

We thank our research and medical staff for making this study possible.

Funding

This work was supported by the National Natural Science Foundation of China (No.82103810) and Outstanding Young Director in Air Force Medical University (4457475042JZ2300U0).

Conflict of Interest

The authors declare no conflict of interest.

References

[1] Eslam M, Newsome PN, Sarin SK, Anstee QM, Targher G, Romero-Gomez M, *et al*. A new definition for metabolic dysfunction-associated fatty liver disease: An international expert consensus statement. Journal of Hepatology. 2020; 73: 202–209. https://doi.org/10.1016/j.jhep.2020.03.039.

[2] Demirtas CO, Yilmaz Y. Metabolic-associated Fatty Liver Disease: Time to integrate ground-breaking new terminology to our clinical practice? Hepatology Forum. 2020; 1: 79–81. https://doi.org/10.14744/hf.2020.2020.0024.

[3] Caussy C, Tripathi A, Humphrey G, Bassirian S, Singh S, Faulkner C, *et al*. A gut microbiome signature for cirrhosis due to nonalcoholic fatty liver disease. Nature Communications. 2019; 10: 1406. https://doi.org/10.1038/s41467-019-09455-9.

[4] Da Silva HE, Teterina A, Comelli EM, Taibi A, Arendt BM, Fischer SE, *et al*. Nonalcoholic fatty liver disease is associated with dysbiosis independent of body mass index and insulin re-

sistance. Scientific Reports. 2018; 8: 1466. https://doi.org/10.1038/s41598-018-19753-9.

[5] Hoyles L, Fernández-Real JM, Federici M, Serino M, Abbott J, Charpentier J, *et al*. Molecular phenomics and metagenomics of hepatic steatosis in non-diabetic obese women. Nature Medicine. 2018; 24: 1070–1080. https://doi.org/10.1038/s41591-018-0061-3.

[6] Schumacher JD, Kong B, Wu J, Rizzolo D, Armstrong LE, Chow MD, *et al*. Direct and Indirect Effects of Fibroblast Growth Factor (FGF) 15 and FGF19 on Liver Fibrosis Development. Hepatology. 2020; 71: 670–685. https://doi.org/10.1002/hep.30810.

[7] Vallianou N, Christodoulatos GS, Karampela I, Tsilingiris D, Magkos F, Stratigou T, *et al*. Understanding the Role of the Gut Microbiome and Microbial Metabolites in Non-Alcoholic Fatty Liver Disease: Current Evidence and Perspectives. Biomolecules. 2021; 12: 56. https://doi.org/10.3390/biom12010056.

[8] Tang H, Zheng Z, Wang H, Wang L, Zhao G, Wang P. Vitamin K2 Modulates Mitochondrial Dysfunction Induced by 6-Hydroxydopamine in SH-SY5Y Cells via Mitochondrial Quality-Control Loop. Nutrients. 2022; 14: 1504. https://doi.org/10.3390/nu14071504.

[9] Ellis JL, Karl JP, Oliverio AM, Fu X, Soares JW, Wolfe BE, *et al*. Dietary vitamin K is remodeled by gut microbiota and influences community composition. Gut Microbes. 2021; 13: 1–16. https://doi.org/10.1080/19490976.2021.1887721.

[10] Su X, Wang W, Fang C, Ni C, Zhou J, Wang X, *et al*. Vitamin K2 Alleviates Insulin Resistance in Skeletal Muscle by Improving Mitochondrial Function *Via* SIRT1 Signaling. Antioxidants & Redox Signaling. 2021; 34: 99–117. https://doi.org/10.1089/ars.2019.7908.

[11] Le Roy T, Llopis M, Lepage P, Bruneau A, Rabot S, Bevilacqua C, *et al*. Intestinal microbiota determines development of non-alcoholic fatty liver disease in mice. Gut. 2013; 62: 1787–1794. https://doi.org/10.1136/gutjnl-2012-303816.

[12] Lan T, Yu Y, Zhang J, Li H, Weng Q, Jiang S, *et al*. Cordycepin Ameliorates Nonalcoholic Steatohepatitis by Activation of the AMP-Activated Protein Kinase Signaling Pathway. Hepatology. 2021; 74: 686–703. https://doi.org/10.1002/hep.31749.

[13] Donohoe DR, Garge N, Zhang X, Sun W, O'Connell TM, Bunger MK, *et al*. The microbiome and butyrate regulate energy metabolism and autophagy in the mammalian colon. Cell Metabolism. 2011; 13: 517–526. https://doi.org/10.1016/j.cmet.2011.02.018.

[14] Cao Y, Vergnes L, Wang YC, Pan C, Chella Krishnan K, Moore TM, *et al*. Sex differences in heart mitochondria regulate diastolic dysfunction. Nature Communications. 2022; 13: 3850. https://doi.org/10.1038/s41467-022-31544-5.

[15] Lee CF, Chavez JD, Garcia-Menendez L, Choi Y, Roe ND, Chiao YA, *et al*. Normalization of NAD+ Redox Balance as a Therapy for Heart Failure. Circulation. 2016; 134: 883–894. https://doi.org/10.1161/CIRCULATIONAHA.116.022495.

[16] Gautheron J, Gores GJ, Rodrigues CMP. Lytic cell death in metabolic liver disease. Journal of Hepatology. 2020; 73: 394–408. https://doi.org/10.1016/j.jhep.2020.04.001.

[17] Karkucinska-Wieckowska A, Simoes ICM, Kalinowski P, Lebiedzinska-Arciszewska M, Zieniewicz K, Milkiewicz P, *et al*. Mitochondria, oxidative stress and nonalcoholic fatty liver disease: A complex relationship. European Journal of Clinical Investigation. 2022; 52: e13622. https://doi.org/10.1111/eci.13622.

[18] Ting S, Jia LI, Qian Z, Xiangni SU. Vitamin K2 alleviates insulin resistance based on gut microbiota. Chinese Journal of Microecology. 2024; 36: 1117–1122. https://doi.org/10.13381/j.cnki.cjm.202410001.

[19] Cani PD, Knauf C. A newly identified protein from Akkermansia muciniphila stimulates GLP-1 secretion. Cell Metabolism. 2021; 33: 1073–1075. https://doi.org/10.1016/j.cmet.2021.05.004.

[20] Choi H, Rao MC, Chang EB. Gut microbiota as a transducer of dietary cues to regulate host circadian rhythms and metabolism. Nature Reviews. Gastroenterology & Hepatology. 2021; 18: 679–689. https://doi.org/10.1038/s41575-021-00452-2.

[21] Buitenhuis HC, Soute BA, Vermeer C. Comparison of the vitamins K1, K2 and K3 as cofactors for the hepatic vitamin K-dependent carboxylase. Biochimica et Biophysica Acta. 1990; 1034: 170–175. https://doi.org/10.1016/0304-4165(90)90072-5.

[22] Booth SL. Vitamin K: food composition and dietary intakes. Food & Nutrition Research. 2012; 56: 5505. https://doi.org/10.3402/fnr.v56i0.5505.

[23] Fu X, Harshman SG, Shen X, Haytowitz DB, Karl JP, Wolfe BE, *et al*. Multiple Vitamin K Forms Exist in Dairy Foods. Current Developments in Nutrition. 2017; 1: e000638. https://doi.org/10.3945/cdn.117.000638.

[24] Lai Y, Masatoshi H, Ma Y, Guo Y, Zhang B. Role of Vitamin K in Intestinal Health. Frontiers in Immunology. 2022; 12: 791565. https://doi.org/10.3389/fimmu.2021.791565.

[25] Suttie JW. The importance of menaquinones in human nutrition. Annual Review of Nutrition. 1995; 15: 399–417. https://doi.org/10.1146/annurev.nu.15.070195.002151.

[26] Shearer MJ, Okano T. Key Pathways and Regulators of Vitamin K Function and Intermediary Metabolism. Annual Review of Nutrition. 2018; 38: 127–151. https://doi.org/10.1146/annurev-nutr-082117-051741.

[27] Beulens JWJ, Booth SL, van den Heuvel EGHM, Stoecklin E, Baka A, Vermeer C. The role of menaquinones (vitamin K_2) in human health. The British Journal of Nutrition. 2013; 110: 1357–1368. https://doi.org/10.1017/S0007114513001013.

[28] Degnan PH, Taga ME, Goodman AL. Vitamin B12 as a modulator of gut microbial ecology. Cell Metabolism. 2014; 20: 769–778. https://doi.org/10.1016/j.cmet.2014.10.002.

[29] Capurso L. Thirty Years of Lactobacillus rhamnosus GG: A Review. Journal of Clinical Gastroenterology. 2019; 53: S1–S41. https://doi.org/10.1097/MCG.0000000000001170.

[30] Lau HCH, Zhang X, Ji F, Lin Y, Liang W, Li Q, *et al*. Lactobacillus acidophilus suppresses non-alcoholic fatty liver disease-associated hepatocellular carcinoma through producing valeric acid. eBioMedicine. 2024; 100: 104952. https://doi.org/10.1016/j.ebiom.2023.104952.

[31] Xie C, Halegoua-DeMarzio D. Role of Probiotics in Non-alcoholic Fatty Liver Disease: Does Gut Microbiota Matter? Nutrients. 2019; 11: 2837. https://doi.org/10.3390/nu11112837.

[32] Otani T, Furuse M. Tight Junction Structure and Function Revisited. Trends in Cell Biology. 2020; 30: 805–817. https://doi.org/10.1016/j.tcb.2020.08.004.

[33] Koentges C, Pfeil K, Schnick T, Wiese S, Dahlbock R, Cimolai MC, *et al*. SIRT3 deficiency impairs mitochondrial and contractile function in the heart. Basic Research in Cardiology. 2015; 110: 36. https://doi.org/10.1007/s00395-015-0493-6.

[34] Sundaresan NR, Gupta M, Kim G, Rajamohan SB, Isbatan A, Gupta MP. Sirt3 blocks the cardiac hypertrophic response by augmenting Foxo3a-dependent antioxidant defense mechanisms in mice. The Journal of Clinical Investigation. 2009; 119: 2758–2771. https://doi.org/10.1172/JCI39162.

[35] Horton JL, Martin OJ, Lai L, Riley NM, Richards AL, Vega RB, *et al*. Mitochondrial protein hyperacetylation in the failing heart. JCI Insight. 2016; 2: e84897. https://doi.org/10.1172/jci.insight.84897.